Chapter 6
Trajectory Planning: Pick-and-Place Operations

6.1 Introduction

The motions undergone by robotic mechanical systems should be, as a rule, as smooth as possible; i.e., abrupt changes in position, velocity, and acceleration should be avoided. Indeed, abrupt motions require unlimited amounts of power to be implemented, which the motors cannot supply because of their physical limitations. On the other hand, abrupt motion changes arise when the robot collides with an object, a situation that should also be avoided. While smooth motions can be planned with simple techniques, as described below, these are no guarantees that no abrupt motion changes will occur. In fact, if the work environment is cluttered with objects, whether stationary or mobile, collisions may occur. Under ideal conditions, a flexible manufacturing cell is a work environment in which all objects, machines and workpieces alike, move with preprogrammed motions that by their nature, can be predicted at any instant. Actual situations, however, are far from being ideal, and system failures are unavoidable. Unpredictable situations should thus be accounted for when designing a robotic system, which can be done by supplying the system with sensors for the automatic detection of unexpected events or by providing for human monitoring. Nevertheless, robotic systems find applications not only in the well-structured environments of flexible manufacturing cells, but also in unstructured environments such as exploration of unknown terrains and systems in which humans are present. The planning of robot motions in the latter case is obviously much more challenging than in the former. Robot motion planning in unstructured environments calls for techniques beyond the scope of those studied in this book, involving such areas as pattern recognition and artificial intelligence. For this reason, we have devoted this book to the planning of robot motions in structured environments only.

Electronic supplementary material The online version of this article (doi: 10.1007/978-3-319-01851-5_6) contains supplementary material, which is available to authorized users.

J. Angeles, *Fundamentals of Robotic Mechanical Systems: Theory, Methods, and Algorithms*, Mechanical Engineering Series 124, DOI 10.1007/978-3-319-01851-5_6,

Two typical tasks call for trajectory planning techniques, namely,

- pick-and-place operations (PPO), and
- continuous paths (CP).

We will study PPO in this chapter, with Chap. 11 devoted to CP. Moreover, we will focus on simple robotic manipulators of the serial type, although these techniques can be directly applied to other, more advanced, robotic mechanical systems.

6.2 Background on PPO

In PPO, a robotic manipulator is meant to take a workpiece from a given *initial pose*, specified by the position of one of its points and its orientation with respect to a certain coordinate frame, to a *final pose*, specified likewise. However, how the object moves from its initial to its final pose is immaterial, as long as the motion is smooth and no collisions occur. Pick-and-place operations are executed in elementary manufacturing operations such as loading and unloading of belt conveyors, tool changes in machine tools, and simple assembly operations such as putting roller bearings on a shaft. The common denominator of these tasks is *material handling*, which usually requires the presence of conventional machines whose motion is very simple and is usually characterized by a uniform velocity. In some instances, such as in *packing operations*, a set of workpieces, e.g., in a magazine, is to be relocated in a prescribed pattern in a container, which constitutes an operation known as *palletizing*. Although palletizing is a more elaborate operation than simple pick-and-place, it can be readily decomposed into a sequence of the latter operations.

It should be noted that although the initial and the final poses in a PPO are prescribed in the Cartesian space, robot motions are implemented in the joint space. Hence, the planning of PPO will be conducted in the latter space, which brings about the need of mapping the motion thus planned into the Cartesian space, in order to ensure that the robot will not collide with other objects in its surroundings. The latter task is far from being that simple, since it involves the rendering of the motion of all the moving links of the robot, each of which has a particular geometry. An approach to path planning first proposed by Lozano-Pérez (1981) consists of mapping the obstacles in the joint space, thus producing obstacles in the joint space in the form of regions that the joint-space trajectory should avoid. The idea can be readily implemented for simple planar motions and simple geometries of the obstacles. However, for general 3-D motions and arbitrary geometries, the computational requirements make the procedure impractical. A more pragmatic approach would consist of two steps, namely, (a) planning a preliminary trajectory in the joint space, disregarding the obstacles, and (b) visually verifying if collisions occur with the aid of a graphics system rendering the animation of the robot motion in the presence of obstacles. The availability of powerful graphics hardware enables the fast animation of robot motions within a highly realistic environment. Shown in Fig. 6.1 is a still image of the animation produced by RVS, the McGill University

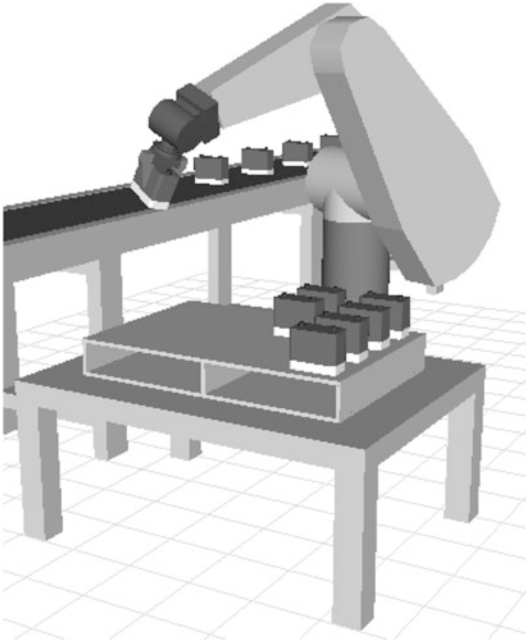

Fig. 6.1 Still image of the animation of a palletizing operation

Robot-Visualization System, of the motion of a robot performing a palletizing operation. Commercial software for robot-motion rendering is available.

By inspection of the kinematic closure equations of robotic manipulators—see Eqs. (4.5a and b)—it is apparent that in the absence of singularities, the mapping of joint to Cartesian variables, and vice versa, is continuous. Hence, a smooth trajectory planned in the joint space is guaranteed to be smooth in the Cartesian space, and the other way around, as long as the trajectory does not encounter a singularity.

In order to proceed to synthesize the joint trajectory, we must then start by mapping the initial and final poses of the workpiece, which is assumed to be rigidly attached to the EE of the manipulator, into manipulator configurations described in the joint space. This is readily done with the methods described in Chap. 4. Let the vector of joint variables at the initial and final robot configurations be denoted by $\boldsymbol{\theta}_I$ and $\boldsymbol{\theta}_F$, respectively. Moreover, the initial pose in the Cartesian space is defined by the position vector $\mathbf{p}_I$ of the operation point P of the EE and a rotation matrix $\mathbf{Q}_I$. Likewise, the final pose in the Cartesian space is defined by the position vector $\mathbf{p}_F$ of P and the rotation matrix $\mathbf{Q}_F$. Moreover, let $\dot{\mathbf{p}}_I$ and $\ddot{\mathbf{p}}_I$ denote the velocity and acceleration of P, while $\boldsymbol{\omega}_I$ and $\dot{\boldsymbol{\omega}}_I$ denote the angular velocity and angular acceleration of the workpiece, all of these at the initial pose. These variables at the final pose are denoted likewise, with the subscript I changed to F. Furthermore, we assume that time is counted from the initial pose, i.e., at this pose, $t = 0$. If the operation takes place in time T, then at the final pose, $t = T$. We have thus the set of conditions that define a smooth motion between the initial and the final poses, namely,

$$\mathbf{p}(0) = \mathbf{p}_I \qquad \dot{\mathbf{p}}(0) = \mathbf{0} \qquad \ddot{\mathbf{p}}(0) = \mathbf{0} \tag{6.1a}$$

$$\mathbf{Q}(0) = \mathbf{Q}_I \qquad \boldsymbol{\omega}(0) = \mathbf{0} \qquad \dot{\boldsymbol{\omega}}(0) = \mathbf{0} \tag{6.1b}$$

$$\mathbf{p}(T) = \mathbf{p}_F \qquad \dot{\mathbf{p}}(T) = \mathbf{0} \qquad \ddot{\mathbf{p}}(T) = \mathbf{0} \tag{6.1c}$$

$$\mathbf{Q}(T) = \mathbf{Q}_F \qquad \boldsymbol{\omega}(T) = \mathbf{0} \qquad \dot{\boldsymbol{\omega}}(T) = \mathbf{0} \tag{6.1d}$$

In the absence of singularities, then, the conditions of zero velocity and acceleration imply zero joint velocity and acceleration, and hence,

$$\boldsymbol{\theta}(0) = \boldsymbol{\theta}_I \qquad \dot{\boldsymbol{\theta}}(0) = \mathbf{0} \qquad \ddot{\boldsymbol{\theta}}(0) = \mathbf{0} \tag{6.2a}$$

$$\boldsymbol{\theta}(T) = \boldsymbol{\theta}_F \qquad \dot{\boldsymbol{\theta}}(T) = \mathbf{0} \qquad \ddot{\boldsymbol{\theta}}(T) = \mathbf{0} \tag{6.2b}$$

6.3 Polynomial Interpolation

A simple inspection of conditions (6.2a) and (6.2b) reveals that a linear interpolation between initial and final configurations will not work here, and neither will a quadratic interpolation, for its slope vanishes only at a single point. Hence, a higher-order interpolation is needed. On the other hand, these conditions imply, in turn, six conditions for every joint trajectory, which means that if a polynomial is to be employed to represent the motion of every joint, then this polynomial should be at least of the fifth degree. We thus start by studying trajectory planning with the aid of a 5th-degree polynomial.

6.3.1 A 3-4-5 Interpolating Polynomial

In order to represent each joint motion, we use here a fifth-order polynomial $s(\tau)$, namely,

$$s(\tau) = a\tau^5 + b\tau^4 + c\tau^3 + d\tau^2 + e\tau + f \tag{6.3}$$

such that

$$0 \leq s \leq 1, \qquad 0 \leq \tau \leq 1 \tag{6.4}$$

and

$$\tau = \frac{t}{T} \tag{6.5}$$

We will thus aim at a *normal polynomial* that, upon scaling both its argument and the polynomial itself, will allow us to represent each of the joint variables θ_j throughout its range of motion, so that

$$\theta_j(t) = \theta_j^I + (\theta_j^F - \theta_j^I)s(\tau) \tag{6.6a}$$

where θ_j^I and θ_j^F are the given initial and final values of the jth joint variable. In vector form, Eq. (6.6a) becomes

$$\boldsymbol{\theta}(t) = \boldsymbol{\theta}_I + (\boldsymbol{\theta}_F - \boldsymbol{\theta}_I)s(\tau) \tag{6.6b}$$

and hence,

$$\dot{\boldsymbol{\theta}}(t) = (\boldsymbol{\theta}_F - \boldsymbol{\theta}_I)s'(\tau)\dot{\tau}(t) = (\boldsymbol{\theta}_F - \boldsymbol{\theta}_I)\frac{1}{T}s'(\tau) \tag{6.6c}$$

Likewise,

$$\ddot{\boldsymbol{\theta}}(t) = \frac{1}{T^2}(\boldsymbol{\theta}_F - \boldsymbol{\theta}_I)s''(\tau) \tag{6.6d}$$

and

$$\dddot{\boldsymbol{\theta}}(t) = \frac{1}{T^3}(\boldsymbol{\theta}_F - \boldsymbol{\theta}_I)s'''(\tau) \tag{6.6e}$$

What we now need are the values of the coefficients of $s(\tau)$ that appear in Eq. (6.3). These are readily found by recalling conditions (6.2a and b), upon consideration of Eqs. (6.6b–d). We thus obtain the end conditions for $s(\tau)$, namely,

$$s(0) = 0, \quad s'(0) = 0, \quad s''(0) = 0, \quad s(1) = 1, \quad s'(1) = 0, \quad s''(1) = 0 \tag{6.7}$$

The derivatives of $s(\tau)$ appearing above are readily derived from Eq. (6.3), i.e.,

$$s'(\tau) = 5a\tau^4 + 4b\tau^3 + 3c\tau^2 + 2d\tau + e \tag{6.8}$$

and

$$s''(\tau) = 20a\tau^3 + 12b\tau^2 + 6c\tau + 2d \tag{6.9}$$

Thus, the first three conditions of Eq. (6.7) lead to

$$f = e = d = 0 \tag{6.10}$$

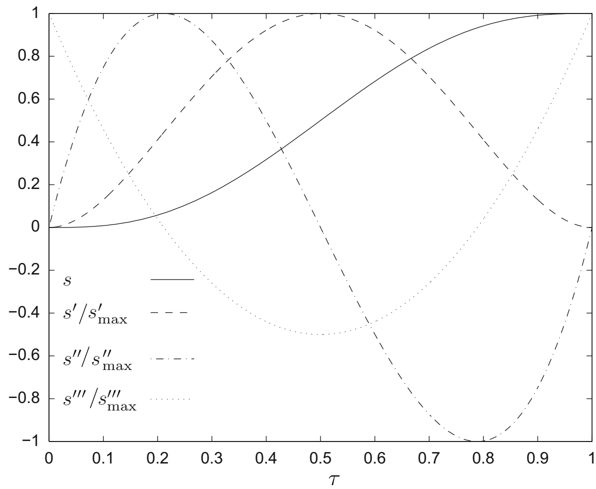

Fig. 6.2 3-4-5 interpolation polynomial and its derivatives

while the last three conditions yield three linear equations in a, b, and c, namely,

$$a + b + c = 1 \tag{6.11a}$$

$$5a + 4b + 3c = 0 \tag{6.11b}$$

$$20a + 12b + 6c = 0 \tag{6.11c}$$

Upon solving the three foregoing equations for the three aforementioned unknowns, we obtain

$$a = 6, \qquad b = -15, \qquad c = 10 \tag{6.12}$$

and hence, the normal polynomial sought is

$$s(\tau) = 6\tau^5 - 15\tau^4 + 10\tau^3 \tag{6.13}$$

which is called a *3-4-5 polynomial.*

This polynomial and its first three derivatives, all normalized to fall within the $(-1, 1)$ range, are shown in Fig. 6.2. Note that the smoothness conditions imposed at the outset are respected and that the curve thus obtained is a monotonically growing function of τ, a rather convenient property for the problem at hand.

It is thus possible to determine the evolution of each joint variable if we know both its end values and the time T required to complete the motion. If no extra conditions are imposed, we then have the freedom to perform the desired motion in as short a time T as possible. Note, however, that this time cannot be given an arbitrarily small value, for we must respect the motor specifications on maximum velocity and maximum torque, the latter being the subject of Chap. 7. In order to ease the discussion, we limit ourselves to specifications of maximum joint velocity and acceleration rather than maximum torque. From the form of function $\theta_j(t)$ of Eq. (6.6a), it is apparent that this function takes on extreme values at points corresponding to those at which the normal polynomial attains its extrema. In order to find the values of τ at which the first and second derivatives of $s(\tau)$ attain maximum values, we need to zero its second and third derivatives. These derivatives are displayed below:

$$s'(\tau) = 30\tau^4 - 60\tau^3 + 30\tau^2 \tag{6.14a}$$

$$s''(\tau) = 120\tau^3 - 180\tau^2 + 60\tau \tag{6.14b}$$

$$s'''(\tau) = 360\tau^2 - 360\tau + 60 \tag{6.14c}$$

from which it is apparent that the second derivative vanishes at the two ends of the interval $0 \leq \tau \leq 1$. Additionally, the same derivative vanishes at the midpoint of the same interval, i.e., at $\tau = 1/2$. Hence, the maximum value of $s'(\tau)$, $s'_{\max}$, is readily found as

$$s'_{\max} = s'\left(\frac{1}{2}\right) = \frac{15}{8} \tag{6.15}$$

and hence, the maximum value of the jth joint rate takes on the value

$$(\dot{\theta}_j)_{\max} = \frac{15(\theta_j^F - \theta_j^I)}{8T} \tag{6.16}$$

which becomes negative, and hence, a local minimum, if the difference in the numerator is negative. The values of τ at which the second derivative attains its extreme values are likewise determined. The third derivative vanishes at two intermediate points τ_1 and τ_2 of the interval $0 \leq \tau \leq 1$, namely, at

$$\tau_{1,2} = \frac{1}{2} \pm \frac{\sqrt{3}}{6} \tag{6.17}$$

and hence, the maximum value of $s''(\tau)$ is readily found as

$$s''_{\max} = s''\left(\frac{1}{2} - \frac{\sqrt{3}}{6}\right) = \frac{10\sqrt{3}}{3} \tag{6.18}$$

while the minimum is given as

$$s''_{\min} = s''\left(\frac{1}{2} + \frac{\sqrt{3}}{6}\right) = -\frac{10\sqrt{3}}{3} \tag{6.19}$$

Therefore, the maximum value of the joint acceleration is as shown below:

$$(\ddot{\theta}_j)_{\max} = \frac{10\sqrt{3}}{3}\frac{(\theta_j^F - \theta_j^I)}{T^2} \tag{6.20}$$

Likewise,

$$s'''_{\max} = s'''(0) = s'''(1) = 60$$

and hence,

$$(\dddot{\theta}_j)_{\max} = 60\frac{\theta_J^F - \theta_j^I}{T^3} \tag{6.21}$$

Thus, Eqs. (6.16) and (6.20) allow us to determine T for each joint so that the joint rates and accelerations lie within the allowed limits. Obviously, since the motors of different joints are different, the minimum values of T allowed by the joints will be, in general, different. Of those various values of T, we will, of course, choose the largest one.

6.3.2 A 4-5-6-7 Interpolating Polynomial

Now, from Eq. (6.14c), it is apparent that the third derivative of the normal polynomial does not vanish at the end points of the interval of interest. This implies that the third time derivative of $\theta_j(t)$, also known as the joint *jerk*, does not vanish at those ends either. It is desirable to have this derivative as smooth as the first two, but this requires us to increase the order of the normal polynomial. In order to attain the desired smoothness, we will then impose two more conditions, namely,

$$s'''(0) = 0, \qquad s'''(1) = 0 \tag{6.22}$$

We now have eight conditions on the normal polynomial, which means that the polynomial degree should be increased to seven, namely,

$$s(\tau) = a\tau^7 + b\tau^6 + c\tau^5 + d\tau^4 + e\tau^3 + f\tau^2 + g\tau + h \tag{6.23a}$$

whose derivatives are readily determined as shown below:

$$s'(\tau) = 7a\tau^6 + 6b\tau^5 + 5c\tau^4 + 4d\tau^3 + 3e\tau^2 + 2f\tau + g \tag{6.23b}$$

$$s''(\tau) = 42a\tau^5 + 30b\tau^4 + 20c\tau^3 + 12d\tau^2 + 6e\tau + 2f \tag{6.23c}$$

$$s'''(\tau) = 210a\tau^4 + 120b\tau^3 + 60c\tau^2 + 24d\tau + 6e \tag{6.23d}$$

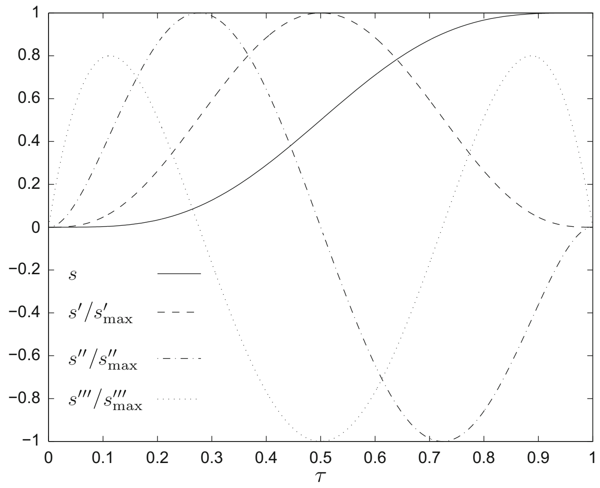

Fig. 6.3 4-5-6-7 interpolating polynomial and its derivatives

The first three conditions of Eq. (6.7) and the first condition of Eq. (6.22) readily lead to

$$e = f = g = h = 0 \tag{6.24}$$

Furthermore, the last three conditions of Eq. (6.7) and the second condition of Eq. (6.22) lead to four linear equations in four unknowns, namely,

$$a + b + c + d = 1 \tag{6.25a}$$

$$7a + 6b + 5c + 4d = 0 \tag{6.25b}$$

$$42a + 30b + 20c + 12d = 0 \tag{6.25c}$$

$$210a + 120b + 60c + 24d = 0 \tag{6.25d}$$

and hence, we obtain the solution

$$a = -20, \qquad b = 70, \qquad c = -84, \qquad d = 35 \tag{6.26}$$

the desired polynomial thus being

$$s(\tau) = -20\tau^7 + 70\tau^6 - 84\tau^5 + 35\tau^4 \tag{6.27}$$

which is a *4-5-6-7 polynomial.* This polynomial and its first three derivatives, normalized to fall within the range $(-1, 1)$, are plotted in Fig. 6.3. Note that the 4-5-6-7 polynomial is similar to that of Fig. 6.2, except that the third derivative of the former vanishes at the extremes of the interval of interest. As we will presently show, this smoothness has been obtained at the expense of higher maximum values of the first and second derivatives.

We now determine the maximum values of the velocity and acceleration produced with this motion. To this end, we display below the first three derivatives, namely,

$$s'(\tau) = -140\tau^6 + 420\tau^5 - 420\tau^4 + 140\tau_3 \quad (6.28a)$$

$$s''(\tau) = -840\tau^5 + 2100\tau^4 - 1680\tau^3 + 420\tau^2 \quad (6.28b)$$

$$s'''(\tau) = -4200\tau^4 + 8400\tau^3 - 5040\tau^2 + 840\tau \quad (6.28c)$$

The first derivative attains its extreme values at points where the second derivative vanishes. Upon zeroing the latter, we obtain

$$\tau^2(-2\tau^3 + 5\tau^2 - 4\tau + 1) = 0 \quad (6.29)$$

which clearly contains a double root at $\tau = 0$. Moreover, the cubic polynomial in the parentheses above admits one real root, namely, $\tau = 1/2$, which yields the maximum value of $s'(\tau)$, i.e.,

$$s'_{\max} = s'\left(\frac{1}{2}\right) = \frac{35}{16} \quad (6.30)$$

whence the maximum value of the jth joint rate is found as

$$(\dot{\theta}_j)_{\max} = \frac{35(\theta_j^F - \theta_j^I)}{16T} \quad (6.31)$$

Likewise, the points of maximum joint acceleration are found upon zeroing the third derivative of $s(\tau)$, namely,

$$s'''(\tau) = -4200\tau^4 + 8400\tau^3 - 5040\tau^2 + 840\tau = 0 \quad (6.32)$$

or

$$\tau(\tau - 1)(5\tau^2 - 5\tau + 1) = 0 \quad (6.33)$$

which yields, in addition to the two end points, two intermediate extreme points, namely,

$$\tau_{1,2} = \frac{1}{2} \pm \frac{\sqrt{5}}{10} \quad (6.34)$$

and hence, the maximum value of acceleration is found to be

$$s''_{\max} = s''(\tau_1) = \frac{84\sqrt{5}}{25} \quad (6.35)$$

the minimum occurring at $\tau = \tau_2$, with $s''_{\min} = -s''_{\max}$. The maximum value of the jth joint acceleration is thus

$$(\ddot{\theta}_j)_{\max} = \frac{84\sqrt{5}}{25}\left(\frac{\theta_j^F - \theta_j^I}{T^2}\right) \tag{6.36}$$

which becomes a minimum if the difference in the numerator is negative. Likewise, the zeroing of the fourth derivative leads to

$$-20\tau^3 + 30\tau^2 - 12\tau + 1 = 0$$

whose three roots are

$$\tau_1 = \frac{1 - \sqrt{3/5}}{2}, \quad \tau_2 = \frac{1}{2}, \quad \tau_1 = \frac{1 + \sqrt{3/5}}{2}$$

and hence,

$$s'''_{\max} = s'''\left(\frac{1 \pm \sqrt{3/5}}{2}\right) = 42, \quad s'''_{\min} = s'''(0.5) = -\frac{105}{2}$$

i.e.,

$$\max_{\tau}\{|s'''(\tau)|\} = \frac{105}{2} \equiv s'''_M \tag{6.37}$$

As in the case of the fifth-order polynomial, it is possible to use the foregoing relations to determine the minimum time T during which it is possible to perform a given PPO while observing the physical limitations of the motors.

6.4 Cycloidal Motion

An alternative motion that produces zero velocity and acceleration at the ends of a finite interval is the *cycloidal motion*. In normal form, this motion is given by

$$s(\tau) = \tau - \frac{1}{2\pi}\sin 2\pi\tau \tag{6.38a}$$

its derivatives being readily derived as

$$s'(\tau) = 1 - \cos 2\pi\tau \tag{6.38b}$$

$$s''(\tau) = 2\pi \sin 2\pi\tau \tag{6.38c}$$

$$s'''(\tau) = 4\pi^2 \cos 2\pi\tau \tag{6.38d}$$

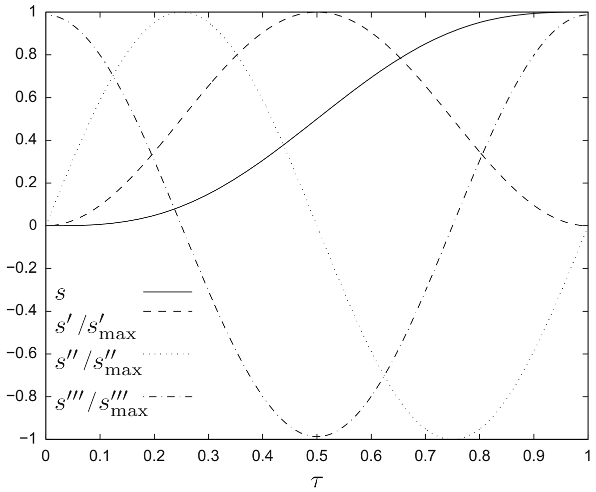

Fig. 6.4 The normal cycloidal motion and its time derivatives

The cycloidal motion and its first three time-derivatives, normalized to fall within the range $(-1, 1)$, are shown in Fig. 6.4. Note that while this motion, indeed, has zero velocity and acceleration at the ends of the interval $0 \leq \tau \leq 1$, its jerk is nonzero at these points and hence, exhibits jump discontinuities at the ends of that interval.

When implementing the cycloidal motion in PPO, we have, for the jth joint,

$$\theta_j(t) = \theta_j^I + (\theta_j^F - \theta_j^I)s(\tau) \tag{6.39a}$$

$$\dot{\theta}_j(t) = \frac{\theta_j^F - \theta_j^I}{T}s'(\tau) \tag{6.39b}$$

$$\ddot{\theta}_j(t) = \frac{\theta_j^F - \theta_j^I}{T^2}s''(\tau) \tag{6.39c}$$

Moreover, as the reader can readily verify, under the assumption that $\theta_j^F > \theta_j^I$, this motion attains its maximum velocity at the center of the interval, i.e., at $\tau = 0.5$, the maximum being

$$s'_{\max} = s'(0.5) = 2$$

and hence,

$$(\dot{\theta}_j)_{\max} = \frac{2}{T}(\theta_j^F - \theta_j^I) \tag{6.40a}$$

Likewise, the jth joint acceleration attains its maximum and minimum values at $\tau = 0.25$ and $\tau = 0.75$, respectively, i.e.,

$$s''_{\max} = s''(0.25) = s''(0.75) = 2\pi \tag{6.40b}$$

and hence,

$$(\ddot{\theta}_j)_{\max} = \frac{2\pi}{T^2}(\theta_j^F - \theta_j^I), \quad (\ddot{\theta}_j)_{\min} = -\frac{2\pi}{T^2}(\theta_j^F - \theta_j^I) \tag{6.40c}$$

Moreover, $s'''(\tau)$ attains its extrema at the ends of the interval, i.e.,

$$s'''_{\max} = s'''(0) = s'''(1) = 4\pi^2 \tag{6.41}$$

and hence,

$$(\dddot{\theta}_j)_{\max} = \frac{4\pi^2}{T^3}(\theta_j^F - \theta_j^I) \tag{6.42}$$

Thus, if motion is constrained by the maximum speed delivered by the motors, the minimum time T_j for the jth joint to produce the given PPO can be readily determined from Eq. (6.40a) as

$$T_j = \frac{2(\theta_j^F - \theta_j^I)}{(\dot{\theta}_j)_{\max}} \tag{6.43}$$

and hence, the minimum time in which the operation can take place can be readily found as

$$T_{\min} = 2 \max_j \left\{ \frac{\theta_j^F - \theta_j^I}{(\dot{\theta}_j)_{\max}} \right\} \tag{6.44}$$

If joint-acceleration constraints are imposed, then a similar procedure can be followed to find the minimum time in which the operation can be realized. As a matter of fact, rather than maximum joint accelerations, maximum joint torques are to be respected. How to determine these torques is studied in detail in Chap. 7.

6.5 Trajectories with via Poses

The polynomial trajectories discussed above do not allow the specification of intermediate Cartesian poses of the EE. All they guarantee is that the Cartesian trajectories prescribed at the initial and final instants are met. One way of verifying the feasibility of the Cartesian trajectories thus synthesized was outlined above and consists of using a graphics system, preferably with animation capabilities, to produce an animated rendering of the robot motion, thereby allowing for verification of collisions. If the latter occur, we can either try alternative branches of the inverse kinematics solutions computed at the end poses or modify the trajectory so as to eliminate collisions. We discuss below the second approach. This is done with what are called *via poses*, i.e., poses of the EE in the Cartesian space that lie between the initial and the final poses, and are determined so as to avoid collisions (Gosselin and Hadj-Messaoud 1993). For example, if upon approaching the final pose of the PPO, the manipulator is detected to interfere with the surface on which the workpiece is to be placed, a via pose is selected close to the final point so that at this pose, the workpiece is far enough from the surface. From inverse kinematics, values of the joint variables can be determined that correspond to the aforementioned via poses. These values can now be regarded as points on the joint-space trajectory and are hence called *via points*. Obviously, upon plotting each joint variable vs. time, via points appear as points on those plots as well.

The introduction of via points in the joint-space trajectories amounts to an increase in the number of conditions to be satisfied by the desired trajectory. For example, in the case of the polynomial trajectory synthesized for continuity up to second derivatives, we can introduce two via points by requiring that

$$s(\tau_1) = s_1, \qquad s(\tau_2) = s_2 \tag{6.45}$$

where τ_1, τ_2, s_1, and s_2 depend on the via poses prescribed and the instants at which these poses are desired to occur. Hence, s_1 and s_2 differ from joint to joint, although the occurrence instants τ_1 and τ_2 are the same for all joints. Thus, we will have to determine one normal polynomial for each joint. Furthermore, the ordinate values s_1 and s_2 of the normal polynomial at via points are determined from the corresponding values of the joint variable determined, in turn, from given via poses through inverse kinematics. Once the via values of the joint variables are known, the ordinate values of the via points of the normal polynomial are found from Eq. (6.6a). Since we have now eight conditions to satisfy, namely, the six conditions (6.7) plus the two conditions (6.45), we need a seventh-order polynomial, i.e.,

$$s(\tau) = a\tau^7 + b\tau^6 + c\tau^5 + d\tau^4 + e\tau^3 + f\tau^2 + g\tau + h \tag{6.46}$$

Again, the first three conditions of Eq. (6.7) lead to the vanishing of the last three coefficients, i.e.,

$$f = g = h = 0 \tag{6.47}$$

Further, the five remaining conditions are now introduced, which leads to a system of five linear equations in five unknowns, namely,

$$a + b + c + d + e = 1 \tag{6.48a}$$

$$7a + 6b + 5c + 4d + 3e = 0 \tag{6.48b}$$

$$42a + 30b + 20c + 12d + 6e = 0 \tag{6.48c}$$

$$\tau_1^7 a + \tau_1^6 b + \tau_1^5 c + \tau_1^4 d + \tau_1^3 e = s_1 \tag{6.48d}$$

$$\tau_2^7 a + \tau_2^6 b + \tau_2^5 c + \tau_2^4 d + \tau_2^3 e = s_2 \tag{6.48e}$$

where τ_1, τ_2, s_1, and s_2 are all data. For example, if the via poses occur at 10 and 90% of T, we have

$$\tau_1 = 1/10, \qquad \tau_2 = 9/10 \tag{6.48f}$$

the polynomial coefficients being found as

$$a = 100(12286 + 12500s_1 - 12500s_2)/729 \tag{6.49a}$$

$$b = 100(-38001 - 48750s_1 + 38750s_2)/729 \tag{6.49b}$$

$$c = (1344358 + 2375000s_1 - 1375000s_2)/243 \tag{6.49c}$$

$$d = (-1582435 - 4625000s_1 + 1625000s_2)/729 \tag{6.49d}$$

$$e = 10(12159 + 112500s_1 - 12500s_2)/729 \tag{6.49e}$$

The shape of each joint trajectory thus depends on the values of s_1 and s_2 found from Eq. (6.6a) for that trajectory.

6.6 Synthesis of PPO Using Cubic Splines

When the number of via poses increases, the foregoing approach may become impractical, or even unreliable. Indeed, forcing a trajectory to pass through a number of via points and meet endpoint conditions is equivalent to interpolation. We have seen that an increase in the number of conditions to be met by the normal polynomial amounts to an increase in the degree of this polynomial. Now, finding the coefficients of the interpolating polynomial requires solving a system of linear equations. As we saw in Sect. 5.8, the computed solution, when solving a system of linear equations, is corrupted with a relative roundoff error that is roughly equal to the relative roundoff error of the data multiplied by an amplification factor that is known as the *condition number* of the system matrix. As we increase the order of the interpolating polynomial, the associated condition number rapidly increases, a fact that numerical analysts discovered some time ago (Kahaner et al. 1989). In order to cope with this problem, *orthogonal polynomials*, such as those bearing the names of *Chebyshev, Laguerre, Legendre*, and so on, have been proposed. While orthogonal polynomials alleviate the problem of a large condition number, they do this only up to a certain extent. As an alternative to higher-order polynomials, *spline functions* have been found to offer more robust interpolation schemes (Dierckx 1993). Spline functions, or *splines*, for brevity, are piecewise polynomials with continuity properties imposed at the *supporting points*. The latter are those points at which two neighboring polynomials join.

The attractive feature of splines is that they are defined as a set of rather lower-degree polynomials joined at a number of supporting points. Moreover, the matrices that arise from an interpolation problem associated with a spline function are such that their condition number is only slightly dependent on the number of supporting points, and hence, splines offer the possibility of interpolating over a virtually unlimited number of points without producing serious numerical conditioning problems.

Below we expand on periodic cubic splines, for these will be shown to be specially suited for path planning in robotics.

A cubic spline function $s(x)$ connecting N points $P_k\ (x_k,\ \ y_k)$, for $k = 1, 2, \ldots, N$, is a *function* defined *piecewise* by $N-1$ cubic polynomials joined at the points P_k, such that $s(x_k) = y_k$. Furthermore, the spline function thus defined is twice differentiable everywhere in $x_1 \le x \le x_N$. Hence, cubic splines are said to be C^2 functions, i.e., to have continuous derivatives up to the second order.

Cubic splines are optimal in the sense that they minimize a *functional*, i.e., an integral defined as

$$F = \int_0^T s''^2(x)\,dx$$

subject to the constraints

$$s(x_k) = y_k, \qquad k = 1, \ldots, N$$

where x_k and y_k are given. The aforementioned optimality property has a simple kinematic interpretation: Among all functions defining a motion so that the plot of this function passes through a set of points $P_1(x_1,\ s_1)$, $P_2(x_2,\ s_2), \ldots, P_N(x_N,\ s_N)$ in the x–s plane, the cubic spline is the one containing the minimum *acceleration magnitude*. In fact, F, as given above, is the square of the *Euclidean norm* (Halmos 1974) of $s''(x)$, i.e., F turns out to be a measure of the *magnitude* of the acceleration of a displacement program given by $s(x)$, if we interpret s as displacement and x as time.

Let $P_k(x_k,\ y_k)$ and $P_{k+1}(x_{k+1},\ y_{k+1})$ be two consecutive supporting points. The kth cubic polynomial $s_k(x)$ between those points is assumed to be given by

$$s_k(x) = A_k\,(x - x_k)^3 + B_k\,(x - x_k)^2 + C_k\,(x - x_k) + D_k \tag{6.50a}$$

for $x_k \le x \le x_{k+1}$. Thus, for the spline $s(x)$, $4(N-1)$ coefficients A_k, B_k, C_k, D_k, for $k = 1, \ldots, N-1$, are to be determined. These coefficients will be computed presently in terms of the given function values $\{s_k\}_1^N$ and the second derivatives of the spline at the supporting points, $\{s_k''(x_k)\}_1^N$, as explained below:

We will need the first and second derivatives of $s_k(x)$ as given above, namely,

$$s_k'(x) = 3A_k(x - x_k)^2 + 2B_k(x - x_k) + C_k \tag{6.50b}$$

$$s_k''(x) = 6A_k(x - x_k) + 2B_k \tag{6.50c}$$

whence the relations below follow immediately:

$$B_k = \frac{1}{2}s_k'' \tag{6.51a}$$

$$C_k = s_k' \tag{6.51b}$$

$$D_k = s_k \tag{6.51c}$$

where we have used the abbreviations

$$s_k \equiv s(x_k), \quad s_k' \equiv s'(x_k), \quad s_k'' \equiv s''(x_k) \tag{6.52}$$

Furthermore, let

$$\Delta x_k \equiv x_{k+1} - x_k \tag{6.53}$$

From the above relations, we have expressions for coefficients B_k and D_k in terms of s_k'' and s_k, respectively, but the expression for C_k is given in terms of s_k'. What we would like to have are similar expressions for A_k and C_k, i.e., in terms of s_k and s_k''. The relations sought will be found by imposing the continuity conditions on the spline function and its first and second derivatives with respect to x at the supporting points. These conditions are, then, for $k = 1, 2, \ldots, N-1$,

$$s_k(x_{k+1}) = s_{k+1} \tag{6.54a}$$

$$s_k'(x_{k+1}) = s_{k+1}' \tag{6.54b}$$

$$s_k''(x_{k+1}) = s_{k+1}'' \tag{6.54c}$$

Upon substituting $s_k''(x_{k+1})$, as given by Eq. (6.50c), into Eq. (6.54c), we obtain

$$6A_k\Delta x_k + 2B_k = 2B_{k+1}$$

but from Eq. (6.51a), we have already an expression for B_k, and hence, one for B_{k+1} as well. Substituting these two expressions in the above equation, we obtain an expression for A_k, namely,

$$A_k = \frac{1}{6\,\Delta x_k}(s_{k+1}'' - s_k'') \tag{6.54d}$$

Furthermore, if we substitute $s_k(x_{k+1})$, as given by Eq. (6.50a), into Eq. (6.54a), we obtain

$$A_k(\Delta x_k)^3 + B_k(\Delta x_k)^2 + C_k\Delta x_k + D_k = s_{k+1}$$

But we already have values for A_k, B_k and D_k from Eqs. (6.54d), (6.51a), and (6.51c), respectively. Upon substituting these values in the foregoing equation, we obtain the desired expression for C_k in terms of function and second-derivative values, i.e.,

$$C_k = \frac{\Delta s_k}{\Delta x_k} - \frac{1}{6}\,\Delta x_k\,(s''_{k+1} + 2s''_k) \tag{6.54e}$$

In summary, then, we now have expressions for all four coefficients of the kth polynomial in terms of function and second-derivative values at the supporting points, namely,

$$A_k = \frac{1}{6\,\Delta x_k}\,(s''_{k+1} - s''_k) \tag{6.55a}$$

$$B_k = \frac{1}{2}\,s''_k \tag{6.55b}$$

$$C_k = \frac{\Delta s_k}{\Delta x_k} - \frac{1}{6}\,\Delta x_k\,(s''_{k+1} + 2s''_k) \tag{6.55c}$$

$$D_k = s_k \tag{6.55d}$$

with

$$\Delta s_k \equiv s_{k+1} - s_k \tag{6.55e}$$

Therefore, in order to find the above coefficients, all we need is the set of values of the second derivatives $\{s''_k\}_1^N$ at the supporting points. To compute these values, we impose the continuity condition on the first derivative, Eq. (6.54b), after substitution of Eq. (6.50b), which yields

$$3A_k(\Delta x_k)^2 + 2B_k\Delta x_k + C_k = C_{k+1}$$

or, if we shift to the previous polynomial,

$$3A_{k-1}(\Delta x_{k-1})^2 + 2B_{k-1}\Delta x_{k-1} + C_{k-1} = C_k$$

Now, if we substitute expressions (6.55a–c) in the above equation, a linear system of $N-2$ simultaneous equations for the N unknowns $\{s''_k\}_1^N$ is obtained, namely,

$$\begin{aligned}(\Delta\ x_k)s''_{k+1} &+ 2(\Delta x_{k-1} + \Delta x_k)s''_k + (\Delta x_{k-1})s''_{k-1}\\ &= 6\left(\frac{\Delta s_k}{\Delta x_k} - \frac{\Delta s_{k-1}}{\Delta x_{k-1}}\right), \quad \text{for} \quad k = 2, \ldots, N-1\,. \end{aligned} \tag{6.56}$$

Further, let $\mathbf{s}$ be the N-dimensional vector whose kth component is s_k, with vector $\mathbf{s}''$ being defined likewise, i.e.,

$$\mathbf{s} = [\, s_1, \cdots, s_N \,]^T, \qquad \mathbf{s}'' = \left[\, s_1'', \cdots, s_N'' \,\right]^T \tag{6.57}$$

The relationship between $\mathbf{s}$ and $\mathbf{s}''$ of Eq. (6.56) can then be written in vector form as

$$\mathbf{A}\,\mathbf{s}'' = 6\,\mathbf{C}\,\mathbf{s} \tag{6.58a}$$

where $\mathbf{A}$ and $\mathbf{C}$ are $(N-2) \times N$ matrices defined as:

$$\mathbf{A} = \begin{bmatrix} \alpha_1 & 2\alpha_{1,2} & \alpha_2 & 0 & \cdots & 0 & 0 \\ 0 & \alpha_2 & 2\alpha_{2,3} & \alpha_3 & \cdots & 0 & 0 \\ \vdots & \vdots & \ddots & \ddots & \ddots & \vdots & \vdots \\ 0 & 0 & \ldots & \alpha_{N'''} & 2\alpha_{N''',N''} & \alpha_{N''} & 0 \\ 0 & 0 & 0 & \cdots & \alpha_{N''} & 2\alpha_{N'',N'} & \alpha_{N'} \end{bmatrix} \tag{6.58b}$$

and

$$\mathbf{C} = \begin{bmatrix} \beta_1 & -\beta_{1,2} & \beta_2 & 0 & \cdots & 0 & 0 \\ 0 & \beta_2 & -\beta_{2,3} & \beta_3 & \cdots & 0 & 0 \\ \vdots & \vdots & \ddots & \ddots & \ddots & \vdots & \vdots \\ 0 & 0 & \cdots & \beta_{N'''} & -\beta_{N''',N''} & \beta_{N''} & 0 \\ 0 & 0 & 0 & \cdots & \beta_{N''} & -\beta_{N'',N'} & \beta_{N'} \end{bmatrix} \tag{6.58c}$$

while for $i, j, k = 1, \ldots, N-1$,

$$\alpha_k \equiv \Delta x_k, \quad \alpha_{i,j} \equiv \alpha_i + \alpha_j, \tag{6.58d}$$

$$\beta_k \equiv 1/\alpha_k, \quad \beta_{i,j} \equiv \beta_i + \beta_j \tag{6.58e}$$

and

$$N' \equiv N - 1, \qquad N'' \equiv N - 2, \qquad N''' \equiv N - 3 \tag{6.58f}$$

Thus, two additional equations are needed to render Eq. (6.58a) a determined system. The additional equations are derived, in turn, depending upon the class of functions one is dealing with, which thus gives rise to various types of splines. For example, if s_1'' and s_N'' are defined as zero, then one obtains *natural cubic splines*, the name arising by an analogy with beam analysis. Indeed, in beam theory, the boundary conditions of a simply-supported beam establish the vanishing of the bending moments at the ends. From beam theory, moreover, the bending moment is proportional to the second derivative of the *elastica*, or *neutral axis*, of the beam with respect to the abscissa along the beam axis in the undeformed configuration. In this case, vector $\mathbf{s}''$ becomes of dimension $N-2$, and hence, matrix $\mathbf{A}$ becomes, correspondingly, of $(N-2) \times (N-2)$, namely,

$$\mathbf{A} = \begin{bmatrix} 2\alpha_{1,2} & \alpha_2 & 0 & \cdots & 0 \\ \alpha_2 & 2\alpha_{2,3} & \alpha_3 & \cdots & 0 \\ \vdots & \ddots & \ddots & \ddots & \vdots \\ 0 & \ldots & \alpha_{N'''} & 2\alpha_{N''',N''} & \alpha_{N''} \\ 0 & 0 & \cdots & \alpha_{N''} & 2\alpha_{N'',N'} \end{bmatrix} \tag{6.59}$$

On the other hand, if one is interested in periodic functions, which is often the case when synthesizing pick-and-place motions, then the conditions $s_1 = s_N$, $s'_1 = s'_N$, $s''_1 = s''_N$ are imposed, thereby producing *periodic cubic splines*. The last of these conditions is used to eliminate one unknown in Eq. (6.58a), while the second condition, namely the continuity of the first derivative, is used to add an equation. We have, then,

$$s'_1 = s'_N \tag{6.60}$$

which can be written, using Eq. (6.54b), as

$$s'_1 = s'_{N-1}(x_N) \tag{6.61}$$

Upon substituting $s'_{N-1}(x_N)$, as given by Eq. (6.50b), into the above equation, we obtain

$$s'_1 = 3A_{N-1}\Delta x^2_{N-1} + 2B_{N-1}\Delta x_{N-1} + C_{N-1} \tag{6.62}$$

Now we use Eqs. (6.55a–c) and simplify the expression thus resulting, which leads to

$$2(\Delta x_1 + \Delta x_{N-1})s''_1 + \Delta x_1 s''_2 + \Delta x_{N-1} s''_{N-1} = 6\left(\frac{\Delta s_1}{\Delta x_1} - \frac{\Delta s_{N-1}}{\Delta x_{N-1}}\right) \tag{6.63}$$

thereby obtaining the last equation required to solve the system of equations given by Eqs. (6.58a–c). We thus have $(N-1)$ independent equations to solve for $(N-1)$ unknowns, namely, s''_k, for $k = 1, \ldots, N-1$, s''_N being equal to s''_1. Expressions for matrices $\mathbf{A}$ and $\mathbf{C}$, as applicable to periodic cubic splines, are given in Eqs. (11.59a and b).

While we focused in the above discussion on cubic splines, other types of splines could have been used. For example, Thompson and Patel (1987) used B-splines in robotics trajectory planning.

Example 6.6.1 (Approximation of a 4-5-6-7 Polynomial with a Cubic Spline). Find the cubic spline that interpolates the 4-5-6-7 polynomial of Fig. 6.3 with $N+1$ equally-spaced supporting points and plot the interpolation error for $N=3$ and $N=10$.

Solution: Let us use a natural spline, in which case the second derivative at the end points vanishes, with vector $\mathbf{s}''$ thus losing two components. That is, we now have only $N-2$ unknowns $\{s''_k\}_2^{N-1}$ to determine. Correspondingly, matrix $\mathbf{A}$ then loses its first and last columns and hence, becomes a square $(N-2)\times(N-2)$ matrix. Moreover,

$$\Delta x_k = \frac{1}{N}, \quad k = 1, \ldots, N$$

and matrices $\mathbf{A}$ and $\mathbf{C}$ become, correspondingly,

$$\mathbf{A} = \frac{1}{N}\begin{bmatrix} 4 & 1 & 0 & \cdots & 0 \\ 1 & 4 & 1 & \cdots & 0 \\ \vdots & \ddots & \ddots & \ddots & \vdots \\ 0 & \ldots & 1 & 4 & 1 \\ 0 & 0 & \cdots & 1 & 4 \end{bmatrix}$$

and

$$\mathbf{C} = N\begin{bmatrix} 1 & -2 & 1 & 0 & \cdots & 0 & 0 \\ 0 & 1 & -2 & 1 & \cdots & 0 & 0 \\ \vdots & \vdots & \ddots & \ddots & \ddots & \vdots & \vdots \\ 0 & 0 & \cdots & 1 & -2 & 1 & 0 \\ 0 & 0 & 0 & \cdots & 1 & -2 & 1 \end{bmatrix}$$

the vector of second derivatives at the supporting points, $\mathbf{s}''$, then being readily obtained as

$$\mathbf{s}'' = 6\mathbf{A}^{-1}\mathbf{C}\mathbf{s}$$

With the values of the second derivatives at the supporting points known, the calculation of the spline coefficients A_k, B_k, C_k, and D_k, for $k = 1, \ldots, N$, is now straightforward. Let the interpolation error, $e(x)$, be defined as $e(x) \equiv s(x) - p(x)$, where $s(x)$ is the interpolating spline and $p(x)$ is the given polynomial. This error and its derivatives $e'(x)$, $e''(x)$, and $e'''(x)$ are plotted in Figs. 6.5 and 6.6 for $N=3$ and $N=10$, respectively. What we observe is an increase of more than one order of magnitude in the error as we increase the order of the derivative by one. Thus, the order of magnitude of acceleration errors is usually higher than two orders of magnitude above the displacement errors, a fact that should not be overlooked in applications.

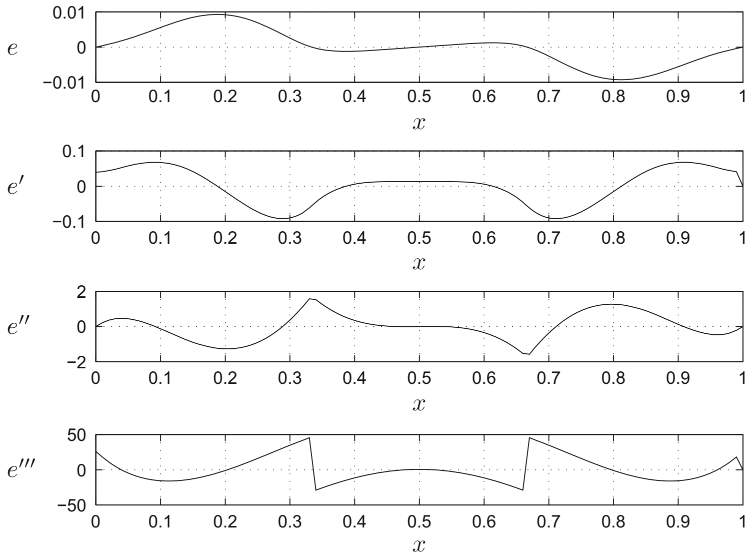

Fig. 6.5 Errors in the approximation of a 4-5-6-7 polynomial with a natural cubic spline, using four supporting points

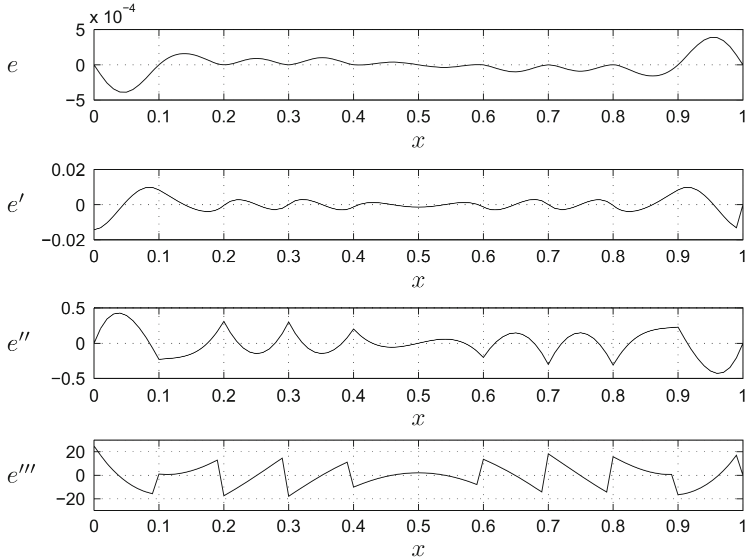

Fig. 6.6 Errors in the approximation of a 4-5-6-7 polynomial with a natural cubic spline, using eleven supporting points

6.7 Exercises

6.1 A common joint-rate program for pick-and-place operations is the trapezoidal profile of Fig. 6.7, whereby we plot $s'(\tau)$ vs. τ, using the notation introduced in Chap. 7, i.e., with $s(\tau)$ and τ defined as dimensionless variables. Here, $s'(\tau)$ starts and ends at 0. From its start to a value τ_1, $s'(\tau)$ grows linearly, until reaching a maximum s'_{max}; then, this function remains constant until a value τ_2 is reached, after which the function decreases linearly to zero at the end of the interval.

Clearly, this profile has a discontinuous acceleration and hence, is bound to produce shock and vibration. However, the profile can be smoothed with a spline interpolation as indicated below.

(a) Find the value of s'_{max} in terms of τ_1 and τ_2 so that $s(0) = 0$ and $s(1) = 1$.
(b) Plot $s(\tau)$ with the value of s'_{max} found above and decompose it into a linear part $s_l(\tau)$ and a periodic part $s_p(\tau)$.
(c) Sample $s(\tau)$ with N equally spaced points and find the *periodic* spline that interpolates $s_p(\tau)$, for $\tau_1 = 0.2$ and $\tau_2 = 0.9$. Try various values of N and choose the one that (a) is the smallest possible, (b) gives a "good" approximation of the original $s(\tau)$, and (c) yields the best-behaved acceleration program, i.e., an acceleration profile that is smooth and within reasonable bounds. Discuss how you would go about defining a reasonable bound.

6.2 An alternative approach to the solution of the foregoing smoothing problem consists in solving an *inverse* interpolation problem: Plot the acceleration program of the foregoing joint-rate plot, $s''(\tau)$. Now, sample a set of N equally spaced points of $s''(\tau)$ and store them in an N-dimensional array $\mathbf{s}''$. Next, find the ordinates of the supporting points of the interpolating *periodic* spline and store them in an array $\mathbf{s}$ of suitable dimension. Note that $\mathbf{s}''$ does not contain information on the linear part of $s(\tau)$. You will have to modify suitably your

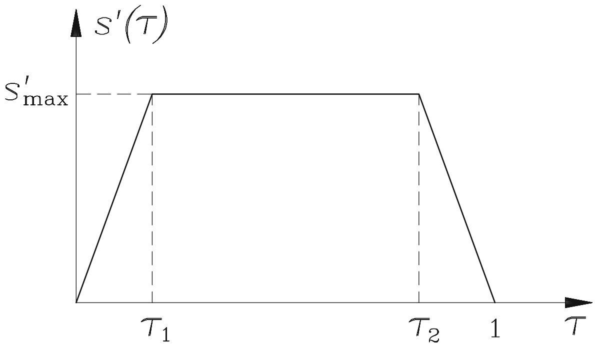

Fig. 6.7 A trapezoidal joint-rate profile

array **s** so that it will produce the correct abscissa values of the interpolated curve $s(\tau)$, with $s(0) = 0$ and $s(1) = 1$. Moreover, $s(\tau)$ must be monotonic. Try various values of N and choose the smallest one that gives a well-behaved acceleration program, as described in Exercise 6.1.

6.3 One more approach to smoothing the joint-rate profile of Fig. 6.7 is to use cycloidal motions. To this end, define a segment of a cycloidal-motion function between $\tau = 0$ and $\tau = \tau_1$, so that $s'(\tau_1) = s'_{\max}$, for $s'_{\max}$ as indicated in the same figure. Further, define a similar segment between $\tau = \tau_2$ and $\tau = 1$ so that $s'(\tau_2) = s'_{\max}$ and $s'(1) = 0$. Then, join the two segments with a line of slope $s'_{\max}$. Plot the displacement, velocity, and acceleration of the smoothed motion. Note that the smoothed profile must meet the end conditions $s(0) = 0$ and $s(1) = 1$, and that you may have to introduce a change of variable to shrink the corresponding $s'(\tau)$ segment to meet these conditions.

6.4 A pick-and-place operation involves picking objects from a magazine supplied with an indexing mechanism that presents the objects with a known pose and zero twist, at equal time-intervals T, to a robot, which is to place the objects on a belt conveyor running at a constant speed v_0. Find 5th- and 7th-degree polynomials that can be suitably used to produce the necessary joint-variable time-histories.

6.5 Repeat Exercise 6.4, but now the objects are to be picked up by the robot from a belt conveyor traveling at a constant velocity $\mathbf{v}_1$ and placed on a second belt conveyor traveling at a constant velocity $\mathbf{v}_2$. Moreover, let $\mathbf{p}_1$ and $\mathbf{p}_2$ designate the position vectors of the points at the pick- and the place poses, respectively. Furthermore, the belts lie in horizontal, parallel planes. Finally, the objects must observe the same attitude with respect to the belt orientation in both the pick- and the place poses.

6.6 Approximate the cycloidal function of Sect. 6.4 using a periodic cubic spline with N subintervals of the same lengths, for various values of N between 5 and 100. Tabulate the approximation error e_N vs. N, with e_N defined as

$$e_N \equiv \max_i \{e_i\}_1^N$$

and

$$e_i \equiv \max_\tau |s(\tau) - c(\tau)|, \quad \tau_i \leq \tau \leq \tau_{i+1}$$

in which $s(\tau)$ denotes the spline approximation and $c(\tau)$ the cycloidal function. *Note: the cycloidal function can be decomposed into a linear and a periodic part.*

6.7 From inspection of the plot of the 3-4-5 polynomial and its derivatives displayed in Fig. 6.2, it is apparent that the polynomial can be regarded as the superposition of a linear and a periodic function in the interval $0 \leq \tau \leq 1$. Approximate the underlying periodic function with a periodic cubic spline by subdividing the above-mentioned interval into N equal subintervals, while finding the value of N that will yield a maximum absolute value of less than 10^{-4} in the error in

(a) the function values;
(b) the values of the first derivative; and
(c) the values of the second derivative.

6.8 Repeat Exercise 6.7 for the 4-5-6-7 polynomial of Fig. 6.3.

6.9 A pick-and-place operation is being planned that should observe manufacturer's bounds on the maximum joint rates delivered by the motors of a given robot. To this end, we have the following choices: (a) a 4-5-6-7 polynomial; (b) a *symmetric* trapezoidal speed profile like that of Fig. 6.7, with $\tau_1 = 0.20$; and (c) a cycloidal motion. Which of these motions produces the minimum time in which the operation can be performed?

6.10 The maximum speed of a cycloidal motion was found to be 2. By noticing that the cycloidal motion is the superposition of a linear and a periodic function, find a cubic-spline motion that will yield a maximum speed of 1.5, with the characteristics of the cycloidal motion at its end points.

6.11 The acceleration of a certain motion $s(\tau)$, for $0 \le \tau \le 1$, is given at a sample of instants $\{\tau_k\}_1^N$ in the form

$$s''(\tau_k) = A \sin(2\pi\tau_k)$$

Find the cubic spline interpolating the given motion so that its second time-derivative will attain those given values, while finding A such that $s(0) = 0$ and $s(1) = 1$. *Hint: A combination of a linear function and a periodic spline can yield this motion. In order to find the function values of the periodic spline, exploit the linear relation between the function values and its second derivatives at the spline supporting points, as discussed in Sect. 6.6.*

6.12 A robotic joint has been found to require to move, within a time-interval T, with a set of speed values $\{\dot{\theta}_k\}_1^N$ at equally spaced instants. Find the natural cubic spline that interpolates the underlying motion so that the angular displacement undergone from beginning to end is a given $\Delta\theta$. *Hint: You will need to establish the linear relation between the spline function values and those of its first derivative.*